ENDOR Spectroscopic Evidence for the Geometry of Binding of *retro-inverso-*N^{ω}-Nitroarginine-Containing Dipeptide Amides to Neuronal Nitric Oxide Synthase

David L. Tierney,‡ Hui Huang,‡ Pavel Martásek,† Linda J. Roman,† Richard B. Silverman,*,‡ and Brian M. Hoffman*,‡

Contribution from the Department of Chemistry and Department of Biochemistry, Molecular Biology, and Cell Biology, Northwestern University, Evanston, Illinois 60208-3113, and Department of Biochemistry, The University of Texas Health Science Center, San Antonio, Texas 78284-7760

Received November 8, 1999

Abstract: We describe in detail the use of 35 GHz Mims pulsed ^{15}N and ^{1,2}H electron−nuclear double resonance (ENDOR) spectroscopy to study the binding of substrates and inhibitors to nitric oxide synthase (NOS). We show that reliable distance estimates, and limited orientation information, can be derived from a small set of data taken near the peak of the absorption mode EPR signal, while more precise orientations require a more extensive data set. The ENDOR approach is then applied to the binding of isoform-selective and non-selective nitroarginine inhibitors. Recently, we reported a family of N^{ω}-nitroarginine-containing dipeptide amides as highly selective inhibitors of nNOS (Huang, H. et al. *J. Med. Chem.* **1999**, *42*, 3147−3153). Two of the most potent analogues were the *retro-inverso*-dipeptide amides L-Arg^{NO_2}-L-Lys-NH_2 (**LL**) and D-Lys-D-Arg^{NO_2}−NH_2 (**DD**). To rationalize the common selectivities of **LL** and **DD**, it was proposed that in both cases the nitroarginine group binds at the heme binding site, therefore requiring one of these molecules to undergo a 180° flip to accommodate such an interaction. The present studies confirm that the dipeptides indeed bind to holo-nNOS quite similarly from the point of view of the nitroguanidine functionality, supporting the earlier interpretation. The data further suggest that a substantial fraction of the **DD** epimer is distributed among other binding geometries.

Nitric oxide synthases (NOS, E. C.1.14.13.39) comprise a family of isozymes that catalyzes the oxidation of L-arginine (**1**) to L-citrulline (**3**) and nitric oxide in an NADPH- and O_2-dependent process (Scheme 1).[1] The first step in the reaction catalyzed by NOS involves *N*-hydroxylation of the guanidino group of L-arginine to give N^{G}-hydroxy-L-arginine (**2**), which is further oxidized in a NADPH- and O_2-dependent reaction to L-citrulline and nitric oxide. The structure of **2** shown in Scheme 1 derives from previous ENDOR studies[2] and recently reported density functional theory calculations.[3]

Two of the isozymes in this family, the neuronal (nNOS) and endothelial (eNOS) forms, are constitutive, and one, the form found in macrophage, is inducible (iNOS).[4] Because a breakdown in the regulation of NO production has been implicated in a wide variety of diseases,[1] inhibition of NOS has the potential of being a useful approach for the treatment of a variety of diseases, but only if inhibition is isoform selective.[5] Recently, we reported the design and synthesis of a series of N^{ω}-nitroarginine-containing dipeptide amides that exhibited remarkable selectivity (hundreds- to thousands-fold) for inhibition of the neuronal isozyme of NOS over the other two isozymes.[6] This nNOS selectivity has implications in the potential treatment of strokes,[7,8] migraine headaches,[9] and Alzheimer's disease.[10] Two of the more selective of the inhibitors reported were L-Arg^{NO_2}-L-Lys-NH_2 (**LL**) and its *retro-inverso* analogue,[11,12] D-Lys-D-Arg^{NO_2}-NH_2 (**DD**). To rationalize the high degree of selectivity for both compounds, the active-site model shown in Figure 1 was proposed.[6] Shemyakin et al.[13]

Scheme 1

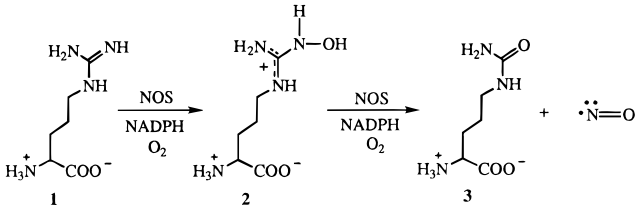

‡ Northwestern University.

† The University of Texas Health Science Center.

(1) Kerwin, J. F. J.; Lancaster, J. R. J.; Feldman, P. L. *Med. Res. Rev.* **1994**, *14*, 23−74.

(2) Tierney, D. L.; Huang, H.; Martásek, P.; Masters, B. S. S.; Silverman, R. B.; Hoffman, B. M. *Biochemistry* **1999**, *38*, 3704−3710.

(3) Tantillo, D. J.; Fukuto, J. M.; Hoffman, B. M.; Silverman, R. B.; Houk, K. N. *J. Am. Chem. Soc.* **2000**, *122*, 536−537.

(4) Stuehr, D. J.; Griffith, O. W. *Adv. Enzymol. Relat. Areas Mol. Biol.* **1992**, *65*, 287−346.

(5) Marletta, M. A. *J. Med. Chem.* **1994**, *37*, 1899−1907.

(6) Huang, H.; Martásek, P.; Roman, L. J.; Masters, B. S. S.; Silverman, R. B. *J. Med. Chem.* **1999**, *42*, 3147−3153.

(7) Choi, D. W.; Rothman, S. M. *Annu. Rev. Neurosci.* **1990**, *13*, 171−182.

(8) Garthwaite, J. in *The NMDA Receptor*; Watkins, J. C., Collingridge, G. L., Eds.; Oxford University Press: Oxford, England, 1989; pp 187−205.

(9) Thomsen, L. L.; Iversen, H. K.; Lassen, L. H.; Olesen, J. *CNS Drugs* **1994**, *2*, 417−422.

(10) Dorheim, M. A.; Tracey, W. R.; Pollock, J. S.; Grammas, P. *Biochem. Biophys. Res. Commun.* **1994**, *205*, 659−665.

(11) Goodman, M.; Chorev, M. *Acc. Chem. Res.* **1979**, *12*, 1−7.

(12) Fletcher, M. D.; Campbell, M. M. *Chem. Rev.* **1998**, *98*, 763−795.

(13) Shemyakin, M. M.; Ovchinnikov, Y. A.; Ivanov, V. T. *Angew. Chem., Int. Ed. Engl.* **1969**, *8*, 492−499.

10.1021/ja993927b CCC: $19.00
Published on Web 08/03/2000

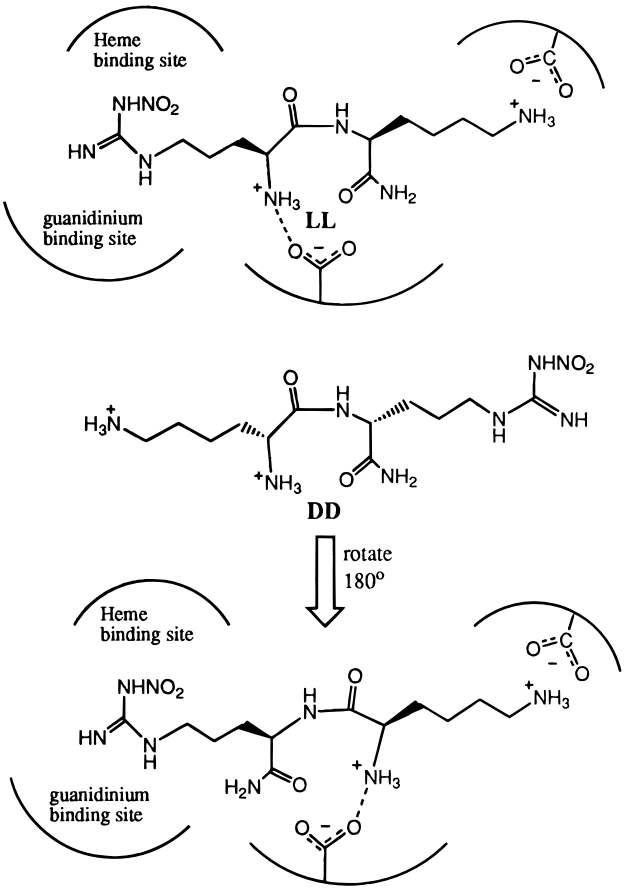

Figure 1. Proposed model for the binding of L-Arg^{NO_2}-L-Lys-NH_2 (**LL**) and D-Lys-D-Arg^{NO_2}−NH_2 (**DD**) to the active site of neuronal NOS.

had proposed a similar kind of model for the binding of two *retro-inverso* peptides to pepsin based on the observation that the K_i value for the D-,D-peptide was similar to the K_m value of the corresponding *retro-inverso* L-,L-peptide substrate. To the best of our knowledge, there is only one report of crystal structures of *retro-inverso* peptides bound to a protein, in this case thermolysin, showing that both peptides bind in the same orientation with their thiolate bound to the active-site zinc ion.[14] The crystal structure of an end group-modified *retro-inverso* isomer of glutathione disulfide bound to glutathione reductase also was obtained to explain why it is a poor substrate for the enzyme.[15]

Electron−nuclear double resonance (ENDOR) spectroscopy has proven to be a sensitive tool for determining the structure of paramagnetic centers in enzyme active sites.[16−18] We recently showed that 35 GHz Mims pulsed ENDOR spectroscopy is surprisingly effective for studying non-covalently bound substrates in the vicinity of the high spin ferriheme of fully functional holo-NOSs, through measurements that determined the binding geometry of L-arginine (L-Arg),[19,20] and both the binding geometry and protonation state of N^G-hydroxy-L-arginine (NOHA).[2,21,22] In the present report, we examine the binding of nitroarginine, ^{15}N-labeled at only the nitro nitrogen (Arg-$^{15}NO_2$) and at both the nitro nitrogen and the guanidino nitrogens (^{15}N-Arg-$^{15}NO_2$), as well as $^{15}NO_2$-**LL** and $^{15}NO_2$-**DD**. We first give a more complete description of the methodology as applied to the structure of nitroarginine bound to holo-nNOS. The resulting framework provided by the structural model for nitroarginine binding is then used to help interpret the data for **LL** and **DD** bound to the functional holo-nNOS, the net result being a confirmation of the proposal depicted in Figure 1, in which the nitroguanidino groups of both **LL** and **DD** are bound at the same binding site as a result of a 180° flip of one of the molecules.

Experimental Section

Preparation of ^{15}N-Labeled Inhibitor Analogues and Inhibitor-nNOS Complexes. The nitro nitrogen in nitroarginine and in the *retro-inverso* dipeptides **LL** and **DD** were labeled with ^{15}N by nitration of L- or D-arginine using $NH_4{}^{15}NO_3$ (Cambridge Isotope Laboratories, Inc., Andover, MA) in H_2SO_4.[23] After Fmoc protection of L- and D-[^{15}N]-nitroarginine, the dipeptide amides **LL** and **DD** were prepared by the previously reported synthetic method.[6] Doubly labeled ^{15}N-nitro-$^{15}N^G$-L-arginine was prepared by the same method via ^{15}N-nitration of commercially available $^{15}N^G$-L-arginine (Cambridge Isotope Laboratories). The appropriately labeled compound was then added, in 20-fold excess, to a solution of holo-nNOS. Samples were prepared for ENDOR spectroscopy as described previously.[19] Samples in D_2O were prepared by two successive 10:1 dilutions in D_2O buffer, followed by reconcentration.

ENDOR Spectra of the Inhibitor−nNOS Complexes. Mims[24] and refocused Mims[25] (Re-Mims) pulsed ENDOR spectra were recorded at 35 GHz with instruments of local design.[26] An important aspect of Mims pulsed-ENDOR is that the absolute intensities, defined as ENDOR intensity per transient divided by ESE intensity and expressed as percent, are well-defined quantities.[27] The ENDOR response from a weakly coupled nucleus with $I = {}^1/_2$ (e.g., ^1H and ^{15}N) is made up of doublets centered at the nuclear Larmor frequency, ν_N, and split by the hyperfine coupling, A. The Mims ENDOR protocol introduces hyperfine selectivity by modulating the ENDOR response according to the relation, $M(\tau) = 1 - \cos 2\pi A\tau$ (where τ is the delay between the first and second microwave pulses), thereby creating blind spots, or "holes," at integral multiples of $A = \tau^{-1}$, as well as a null at $A = 0$.[24] The Mims ENDOR response is governed by the interplay of two governing factors: the exponential decay of the ESE with increasing τ, and the $M(\tau)$ hyperfine selectivity of the Mims pulse sequence. Resonances from the ^{15}N of labeled substrates/inhibitors appear in a region where they overlap with ^{14}N resonances from the pyrrole nitrogens. However, in all spectra, $A(^{15}N) \ll \tau^{-1}$, while for the pyrrole nitrogens, $A(^{14}N) \gg \tau^{-1}$. As a result, the Mims hyperfine selectivity attenuates the response of the ^{14}N and affords a clean spectral window

(14) Roderick, S. L.; Fourniezaluski, M. C.; Roques, B. P.; Matthews, B. W. *Biochemistry* **1989**, *28*, 1493−1497.
(15) Janes, W.; Schulz, G. E. *J. Biol. Chem.* **1990**, *265*, 10443−5.
(16) Hoffman, B. M.; DeRose, V. J.; Doan, P. E.; Gurbiel, R. J.; Houseman, A. L. P.; Telser, J. *Biological Magnetic Resonance*; Berliner, L. J., Reuben, J., Eds.; Metalloenzyme Active-Site Structure and Function through Multifrequency CW and Pulsed ENDOR, Vol. 13; Plenum Press: New York and London, 1993; pp 151−218.
(17) DeRose, V. J.; Hoffman, B. M. *Methods in Enzymology*; Sauer, K., Ed.; Protein Structure and Mechanism Studied by Electron Nuclear Double Resonance Spectroscopy, Vol. 246; Academic Press: New York, 1995; pp 554−589.
(18) Mustafi, D.; Joela, H.; Makinen, M. W. *J. Magn. Reson.* **1991**, *91*, 497−504.
(19) Tierney, D. L.; Martásek, P.; Doan, P. E.; Masters, B. S.; Hoffman, B. M. *J. Am. Chem. Soc.* **1998**, *120*, 2983−2984.
(20) Tierney, D. L.; Huang, H.; Martásek, P.; Roman, L. J.; Silverman, R. B.; Masters, B. S. S.; Hoffman, B. M. *J. Am. Chem. Soc.* **2000**, *122*, 5405−5406.
(21) Crane, B. R.; Arvai, A. S.; Ghosh, S.; Getzoff, E. D.; Stuehr, D. J.; Tainer, J. A. *Biochemistry* **2000**, *39*, 4608−4621.
(22) A recent low-resolution (2.6 Å) crystal structure of the iNOS oxygenase domain complexed with NOHA showed that the N of the NOHA "N−OH" moiety is roughly above the heme Fe, thereby leading to the ENDOR-based conclusion that this is, in fact, an "NH−OH" moiety.
(23) Hayakawa, T.; Fujiwara, Y.; Noguchi, J. *Bull. Chem. Soc. Jpn.* **1967**, *40*, 1205−1208.
(24) Mims, W. B. *Proc. R. Soc. London* **1965**, *283*, 452−457.
(25) Doan, P. E.; Hoffman, B. M. *Chem. Phys. Lett.* **1997**, *269*, 208−214.
(26) Davoust, C. E.; Doan, P. E.; Hoffman, B. M. *J. Magn. Reson.* **1996**, *119*, 38−44.
(27) Doan, P. E.; Fan, C.; Hoffman, B. M. *J. Am. Chem. Soc.* **1994**, *116*, 1033−1041.

for the observation of weakly coupled ^{15}N. In these measurements, τ is chosen to optimize the absolute ENDOR response of ^{15}N or ^{1}H, rather than concerns about the proximity of a resonance to a "hole" (see Figure 5B).

Because substrates and inhibitors bind near to the NOS ferriheme, without coordinating to it, the observed hyperfine coupling to ^{15}N and ^{1}H nuclei of the substrate or inhibitor is determined by the dipolar interaction with the high spin Fe^{3+}. The intrinsic dipolar interaction between the $S = {}^5/_2$ ferric ion and a substrate/inhibitor nucleus has axial symmetry, $\mathbf{T} = [-T_\perp, -T_\perp, T_{||}] = [-T, -T, 2T]$, where the unique direction corresponds to the metal-nucleus vector, and the magnitude of the perpendicular component is given by eq 1.

$$T = \rho_{Fe} g_e g_N \beta_e \beta_N / r^3 \quad (1)$$

In eq 1, g_N and g_e are the nuclear and electronic g factors, respectively, β_e and β_N are the electronic and nuclear magnetons, and r is the metal−nucleus distance. The fraction of the total electron spin (five unpaired electrons) on iron, ρ_{Fe}, (defined as $\rho_{Fe} = 1$ for a purely ionic Fe^{3+}) was estimated by determining the spin density in the sigma orbitals of the pyrrole nitrogens through analysis of the $^{14}N_{pyrrole}$ isotropic couplings (A_{iso} = 8−8.5 MHz for each nitrogen, Figure S1) as described earlier.[28,29] This treatment gives roughly 7−8% of one electron spin on each of the four pyrrole nitrogens. Assuming that ∼10% of one electron (2% of the total spin) resides on the axial cysteine thiolate, then ∼40% of an electron, or ∼8% of the total spin, is delocalized onto ligand atoms; given the existence of small spin densities on other heme atoms this was rounded to 10%, giving ρ_{Fe} ∼0.9. This value has subsequently been verified through comparison of ENDOR-derived distances to crystallographically derived ones.[2] The strong g anisotropy of the nNOS ferriheme scales the hyperfine coupling by the observing g-value; for example, when the metal-nucleus vector lies along g_3, then the dipolar interaction has principal values of $\mathbf{T}' = [T_1', T_2', T_3'] = [-(g_1/g_e)T, -(g_2/g_e)T, 2(g_3/g_e)T]$. Equations for the general case are available[30] and are incorporated in the programs used here for detailed analyses.[31] A particularly useful characteristic of the dipolar interaction is that even for appreciable deviations from coaxiality of **g** and **T**, the ENDOR spectrum obtained at the peak of the absorption mode EPR signal (g_2) is dominated by a doublet whose splitting is closely approximated by T_2'. As a result, in general, the metal-nucleus distance, r, can be determined directly from the measured doublet splitting at g_2.

The orientation of the metal-nucleus vector relative to the g-tensor can be accurately determined through simulation of the full 2D field-frequency plot generated by collecting ENDOR spectra at numerous fields across the EPR envelope.[16,17] This permits evaluation of the hyperfine tensor, **A**, both its principal values and its orientation. Fits to such data allow for the possibility of an isotropic coupling term, as well as the anisotropic dipolar term. However, in the present work, where we examine non-covalently bound substrates and inhibitors, this term is uniformly small. A rough estimate of the angular position of the substrate ^{15}N can be obtained by analyzing the line shape at g_2, specifically the breadth and intensity of the shoulders outside the central doublet (see, for example, Figure 3). Only at relatively large values of θ (rotation of A_z away from g_z), are the spectra no longer dominated by $A_\perp$, and then a determination of r requires a more complete field dependent analysis. For small θ (≤5°), the parameter ϕ is largely undetermined, due to the axial nature of the dipolar interaction. It is important to note that, in this case (rhombic **g**, axial **A**), the observed doublet splitting in the "single-crystal-like" ENDOR spectrum taken at the low-field (high-g) edge of the EPR envelope is highly dependent on the angular parameters. In general, and in contrast to the g_2 region, the distance r cannot be estimated reliably from the low-field spectra.

(28) Brown, T. G.; Hoffman, B. M. *Mol. Phys.*, **1980**, *39*, 1073−1109.
(29) Scholes, C. P.; Lapidot, A.; Mascarenhas, R.; Inubushi, T.; Isaacson, R. A.; Feher, G. *J. Am. Chem. Soc.*, **1982**, *104*, 2724−2735.
(30) Hutchison, C. A., Jr.; McKay, D. B. *J. Chem. Phys.* **1977**, *66*, 3311−3330.
(31) The ENDOR simulation programs, GENDOR and GENSIM, can be obtained free of charge from our website <http://endor1.chem.northwestern.edu/program1.htm>.

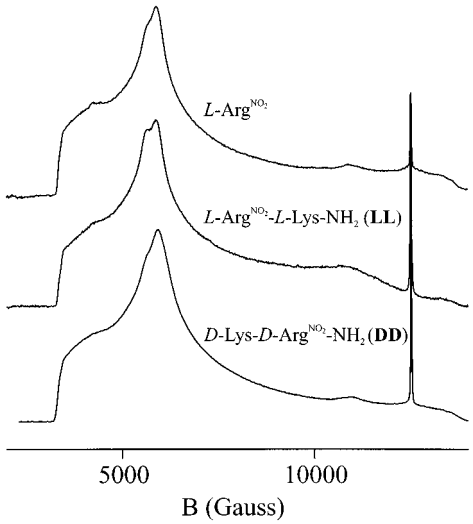

Figure 2. Absorption mode 35 GHz CW EPR spectra for holo-nNOS with bound nitroarginine, with bound L-Arg^{NO_2}-L-Lys-NH_2 (**LL**), and with bound D-Lys-D-Arg^{NO_2}-NH_2 (**DD**). Conditions: ν_{MW} = 35.0 GHz, MW power = 50 μW, 2 G field modulation (100 kHz), time constant = 32 ms, receiver gain = 80.

Results

EPR Spectra. Absorption mode 35 GHz CW EPR spectra of nNOS in the presence of L-nitroarginine and the dipeptide amide inhibitors, **LL** and **DD**, are presented in Figure 2. The spectra are characteristic of the $\pm{}^1/_2$ doublet of an $S = {}^5/_2$, high-spin d^5 system with large zero field splitting. Previous EPR studies[32] have shown that binding of substrates, L-Arg and NOHA, quantitatively shift the EPR signal of the nNOS ferriheme from that of a six-coordinate, low spin Fe^{3+} to a that of a five-coordinate, highly rhombic high-spin Fe^{3+} with $g_{1,2,3}$ = [7.56, 4.19, 1.81] for L-Arg and [7.65, 4.03, 1.81] for NOHA. Binding of L-nitroarginine causes a similar shift in the ferriheme spin equilibrium, although the resultant high spin state is slightly less rhombic.[32] Our measurements for the L-nitroarginine complex give **g** = [7.39, 4.28, 1.88]; the value of g_2 given here for the nitroarginine complex is smaller than that previously reported (g_2 = 4.43)[32] and was deduced from simulations of the ^{15}N ENDOR pattern (discussed below). The spectra for the two dipeptide complexes also are quantitatively shifted to a high-spin form with the same g-tensor seen for L-nitroarginine.

Mims ^{15}N Pulsed-ENDOR Spectra at g_2. ^{15}N ENDOR spectra for $^{15}N^{G}$-L-arginine (^{15}N-Arg), $^{15}N^{nitro}$-L-nitroarginine (Arg-$^{15}NO_2$), $^{15}N^{nitro}$-**LL** ($^{15}NO_2$-**LL**), and $^{15}N^{nitro}$-**DD** ($^{15}NO_2$-**DD**) bound to holo-nNOS, taken at g_2 = 4.28 (except for ^{15}N-Arg, where g_2 = 4.19), are presented in Figure 3. All of the spectra display the T_2' doublet, from which one directly calculates the value of r_{Fe-N} given in Table 1. For Arg-$^{15}NO_2$, the observed splitting at g_2 is A = 0.19 MHz, slightly smaller than the 0.22 MHz observed for ^{15}N-Arg. This indicates that the nitro nitrogen of Arg-$^{15}NO_2$ is farther from the heme iron (r_{Fe-N} = 4.3 Å) than the guanidino nitrogen of ^{15}N-Arg (r_{Fe-N} = 4.1 Å). The similarity of the line shapes for the two compounds indicates that both nitrogens occupy similar positions with respect to the ferric ion's g-tensor (below).

The two dipeptides show ^{15}N T_2' signatures at g_2 that are indistinguishable from that of Arg-$^{15}NO_2$, indicating that the distance to the nitro nitrogen is the same for the dipeptides as it is for nitroarginine (Table 1). This result establishes that the

(32) Salerno, J. C.; McMillan, K.; Masters, B. S. S. *Biochemistry* **1996**, *35*, 11839−11845.

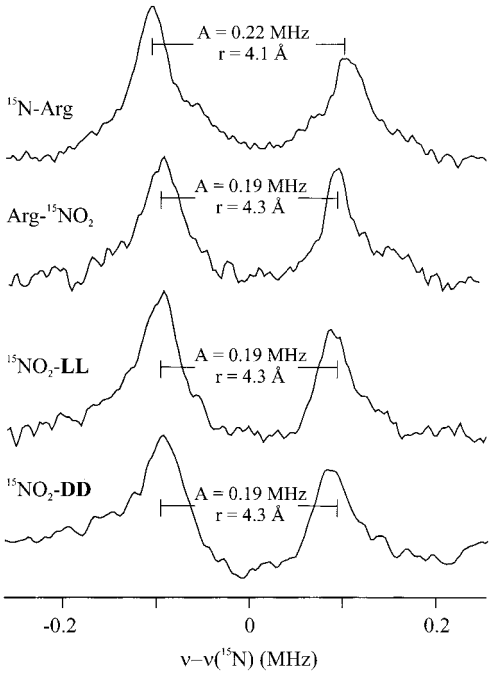

Figure 3. Comparison of 35 GHz Mims pulsed-ENDOR spectra at g_2 for holo-nNOS with bound ^{15}N-Arg, Arg-^{15}NO$_2$, ^{15}NO$_2$-**LL** and ^{15}NO$_2$-**DD** ($g_2 = 4.28$, except for ^{15}N-Arg, where $g_2 = 4.19$). Conditions: $T = 2$ K, $\nu_{MW} = 34.70$ GHz, MW pulse lengths = 40 ns, $\tau = 700$ ns, RF pulse length = 40 μs, repetition rate = 200 Hz. Each spectrum consists of 256 points, with each point an average of 2000 transients.

Table 1. ENDOR-derived Structural Parameters for ^{15}N-labeled Substrate and Inhibitors Bound to nNOS

	T_2'[a]	r_{Fe-N}[b] (Å)	θ[c] (deg)	ϕ[d] (deg)	% I[e]	fwhm[f]	Δr[g]
^{15}N-Arg	0.22	4.1	15	45	2.8	44	0.12
Arg-^{15}NO$_2$	0.19	4.3	15	45	2.6	46	0.14
^{15}NO$_2$-**LL**	0.19	4.3	15	45	2.3	51	0.16
^{15}NO$_2$-**DD**	0.19	4.3	15	45	1.4	49	0.15
^{15}N-Arg-^{15}NO$_2$	0.19	–	–	–	5.0	43	0.13
guanidino ^{15}N	0.19	4.3	0	0			
nitro ^{15}N	0.19	4.3	15	45			

[a] Doublet splitting at g_2 in MHz (±0.01 MHz). [b] Calculated from eq 1 (±0.1 Å). [c] Rotation of A_z away from g_z, ±5°. [d] Rotation of **A** in the $g_{x,y}$ plane, ±10°. [e] Percent ENDOR effect, defined as: ((ENDOR intensity/transient)/(ESE intensity/transient)) × 100. [f] fwhm in kHz. [g] Calculated using fwhm in eq 1: $r(T_2' + {}^1/_2\,\text{fwhm}) - r(T_2' - {}^1/_2\,\text{fwhm})$.

dipeptides **LL** and **DD** both bind with the nitroarginine moiety in the same location, adjacent to the heme iron, consistent with the model depicted in Figure 1. The ^{15}N doublets at g_2 for ^{15}N-Arg and the three inhibitors all show sharp peaks, with full width at half-maximum (fwhm) <51 kHz. The appearance of such sharp lines requires that the nitro nitrogen must be held in a very well-defined position in *all* cases. Attributing this entire breadth to positional disorder (ΔA) gives an upper limit to the spread in distances of $\Delta r \approx 0.15$ Å. A formal treatment of the distribution problem, to be published, confirms this approximation.

Analysis of 2D Data for ^{15}N-labeled Substrates/Inhibitors Bound to nNOS. Two-dimensional field-frequency ^{15}N ENDOR data were collected for Arg-^{15}NO$_2$ over the extended field range of $g = 4.07-7.39$ (Figure 4). Additional data outside of this range could not be obtained because of diminished ESE intensity. Simulations of the field dependent ^{15}N pattern show that the maximum intensity of the perpendicular component of the observed hyperfine is expected to occur at exactly g_2.

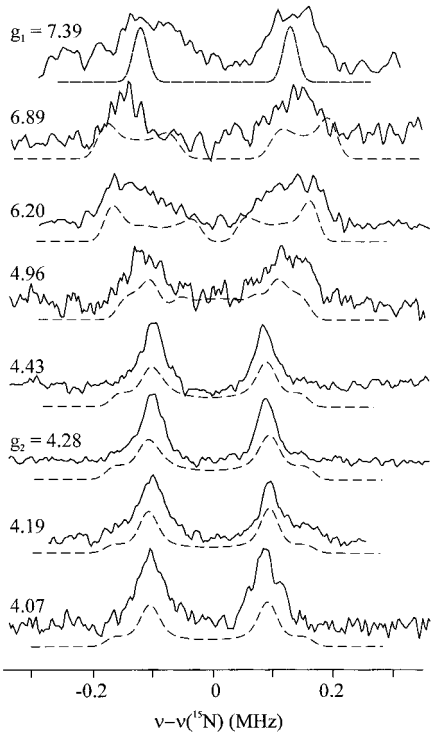

Figure 4. Field dependent35 GHz Mims pulsed-ENDOR spectra for holo-nNOS with bound ^{15}N-nitro-L-arginine (Arg-^{15}NO$_2$). Conditions: Same as in Figure 3. The dotted lines are simulations based on an Fe−N distance of 4.3 Å, with Euler angles of $\theta = 15°$ and $\phi = 45°$. The simulations include 15 kHz of isotropic hyperfine coupling.

Examination of the normalized ENDOR intensities shows that the maximum for nitroarginine occurs at $g_2 = 4.28$, hence our reassignment of this value. At fields outside the window near g_2, the pattern changes appreciably with field, as orientations with hyperfine couplings other than T_2' begin to contribute proportionately greater intensity. Thus, simulations of the entire set of 2D ^{15}N data for Arg-^{15}NO$_2$ give reliable orientational information, as well as the metal-nucleus distance. The best fit to the data, shown as overlays to the experimental data in Figure 4, indicates that the Fe−N vector is 4.3 Å in length and subtends a 15(5)° angle with the heme normal (θ), lying roughly between the Fe−N$_{pyrrole}$ bonds in the heme plane ($\phi = 45(10)°$). The Euler angles for Arg-^{15}NO$_2$ obtained from the field-dependent data are identical to those for ^{15}N-Arg.[20]

This extended data set can be used to examine the expectation that spectra near g_2 are sufficient to determine the metal−nucleus distance to good accuracy, as well as to provide limited orientation information. While data at g_2, and often over a range of fields around g_2, is easily obtained, more extensive data often cannot be acquired due to the loss of ESE intensity at fields away from g_2. As seen in Figure 4, the sharp T_2' doublet dominates not only the ENDOR spectrum taken at g_2, but also those taken within a range of fields around g_2 ($4.07 \le g \le 4.43$). The splitting of this doublet is relatively field independent, confirming that it is a robust measurement of T_2' and thus r_{Fe-N}. Fitting only the spectrum at g_2, we could place the following limits on the position of the nitro nitrogen of Arg-^{15}NO$_2$: $r_{Fe-N} = 4.3$ Å, $\theta = 5-25°$, $\phi = 15-75°$. Fitting the spectra between $g = 4.07-4.43$ gives $r_{Fe-N} = 4.3$ Å, $\theta = 10-20°$ and $\phi = 25-65°$. Comparing these values to those obtained from fitting the full 2D data set of Figure 4 ($r_{Fe-N} = 4.3$ Å, $\theta = 15(5)°$, $\phi = 45(10)°$), one sees that r, and also θ, are very well determined by the spectra at and near g_2, but the more extended data set is necessary to determine the best value of ϕ.

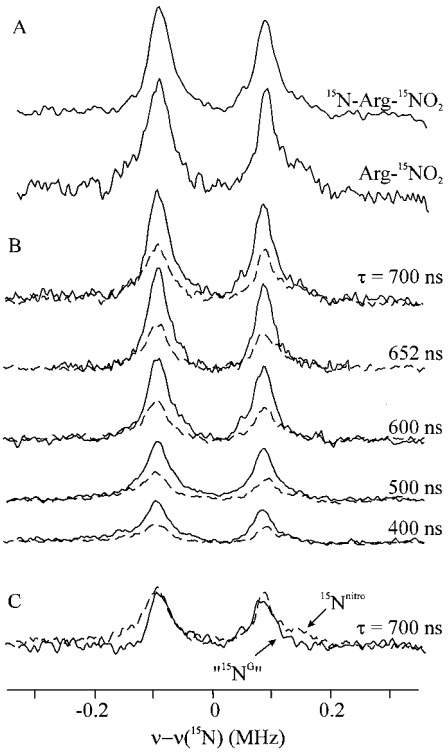

Figure 5. Comparison of 35 GHz Mims pulsed-ENDOR spectra at $g_2 = 4.28$ for holo-nNOS with bound ^{15}N-Arg-^{15}NO$_2$ and with bound Arg-^{15}NO$_2$. **(A)** Spectra at $\tau = 700$ ns, scaled to the same height. **(B)** Dependence of absolute ENDOR intensity on the interpulse delay, τ, for the ^{15}N-Arg-^{15}NO$_2$ (solid) and Arg-^{15}NO$_2$ (dashed) complexes of nNOS. **(C)** Absolute intensity "^{15}N^{G}" spectrum obtained as the (^{15}N-Arg-^{15}NO$_2$) − (Arg-^{15}NO$_2$) difference at $\tau = 700$ ns (solid). The overlay (dashed) is the Arg-^{15}NO$_2$ spectrum at $\tau = 700$ ns. This comparison clearly shows that the outer shoulders belong to the nitro nitrogen. Conditions: Same as in Figure 3.

Scheme 2

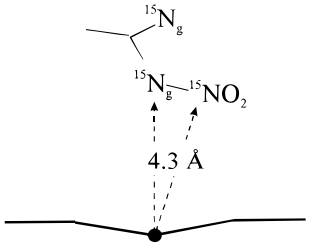

The Structure of Nitroarginine Bound to nNOS. To further refine the binding geometry of nitroarginine, a sample was prepared with doubly ^{15}N labeled nitroarginine (^{15}N-Arg-^{15}NO$_2$). When scaled to the same height, the ^{15}N ENDOR spectra at g_2 for doubly labeled nitroarginine and for singly labeled nitroarginine bound to nNOS (Figure 5A) appear indistinguishable, from which one might infer that the guanidino ^{15}N does not give a detectable signal, perhaps because it is farther from the heme iron. However, closer examination of the absolute ENDOR intensities, taken over a range of τ (Figure 5B), reveals that, in fact, the doubly ^{15}N-labeled sample quantitatively gives double the ENDOR response of singly ^{15}N-labeled nitroarginine. The ratio of the peak *intensities* for the two compounds ranges from 2.3 at short τ, to 2.1 at long τ, reflecting differences in the intensity of the outer shoulders on the two ^{15}N doublets. Numerical integration of the spectra ($\nu_N \pm 0.3$ MHz) shows that the ratio of peak *areas* is 2 ± 0.1 for all values of τ. Clearly, the T_2' doublet for the doubly labeled sample reflects equal

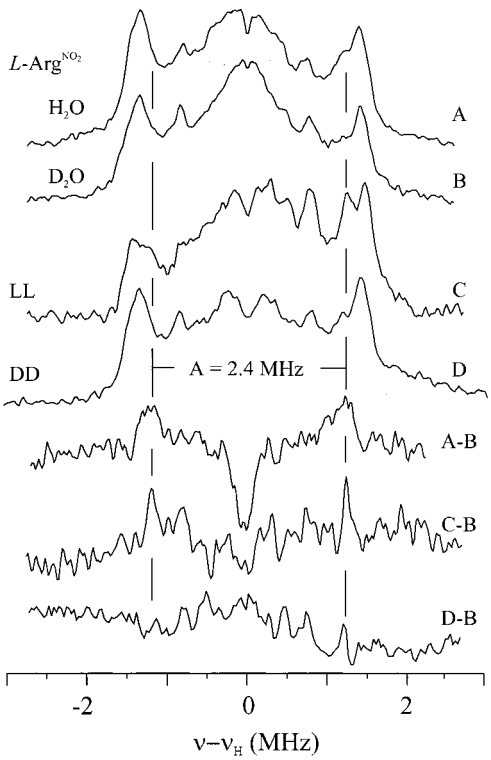

Figure 6. 35 GHz refocused Mims ^{1}H ENDOR spectra taken at $g_1 = 7.39$ for nitroarginine in (A) H_2O and (B) D_2O, for (C) **LL**, and for (D) **DD** bound to holo-nNOS, and their difference spectra. Conditions: $\tau = 140$ ns, MW pulse lengths = 28, 28, 28, and 60 ns, 3000 transients; other conditions as in Figure 3.

contributions from *both* the nitro ^{15}N and one of the guanidino ^{15}Ns. For a given field and τ, therefore, the difference between the spectra for the doubly and singly labeled samples corresponds to the spectrum for the guanidino ^{15}N (Figure 5C).

Observation of a *pair* of ^{15}N nuclei from doubly labeled nitroarginine, each with a perpendicular hyperfine coupling of ~0.19 MHz requires that both the nitro nitrogen and the guanidino nitrogen to which it is attached are essentially equidistant from the heme iron. To determine the minimum spread in r_{Fe-N} necessary to resolve a pair of ^{15}N doublets, a series of simulations were performed, varying the difference in the two iron−nitrogen distances (Δr) while holding all other parameters fixed. The results of these simulations are summarized in Table S1. Comparison of the calculated fit residuals shows that the best simulation is for a distance difference of 0.1−0.2 Å. The same trend is apparent in the simulated line widths (Table S1).

Although T_2', and thus r_{Fe-N}, for the two ^{15}N of ^{15}N-Arg-^{15}NO$_2$ is essentially the same, the orientations are not. Comparison between data for doubly labeled ^{15}N-Arg-^{15}NO$_2$ and data for singly labeled Arg-^{15}NO$_2$ (double ^{15}N − single ^{15}N, Figure 5C) shows that all of the intensity in the outer shoulders on the ^{15}N doublet for the doubly labeled compound must be attributed to the nitro nitrogen. These shoulders appear because of a significant displacement of the nitro nitrogen from the heme normal ($\theta \approx 15°$). The absence of outer shoulders on the doublet for the guanidino nitrogen indicates this ^{15}N lies almost exactly on the heme normal ($\theta \approx 0°$). The field dependence of the difference spectra (Figure S2 and S3), which should correspond to the spectra for the guanidino ^{15}N, were fit to determine r_{Fe-N}, θ and ϕ for this nitrogen. The best orientational parameters for the individual nitrogens (Table 1) predict the binding geometry depicted in Scheme 2.

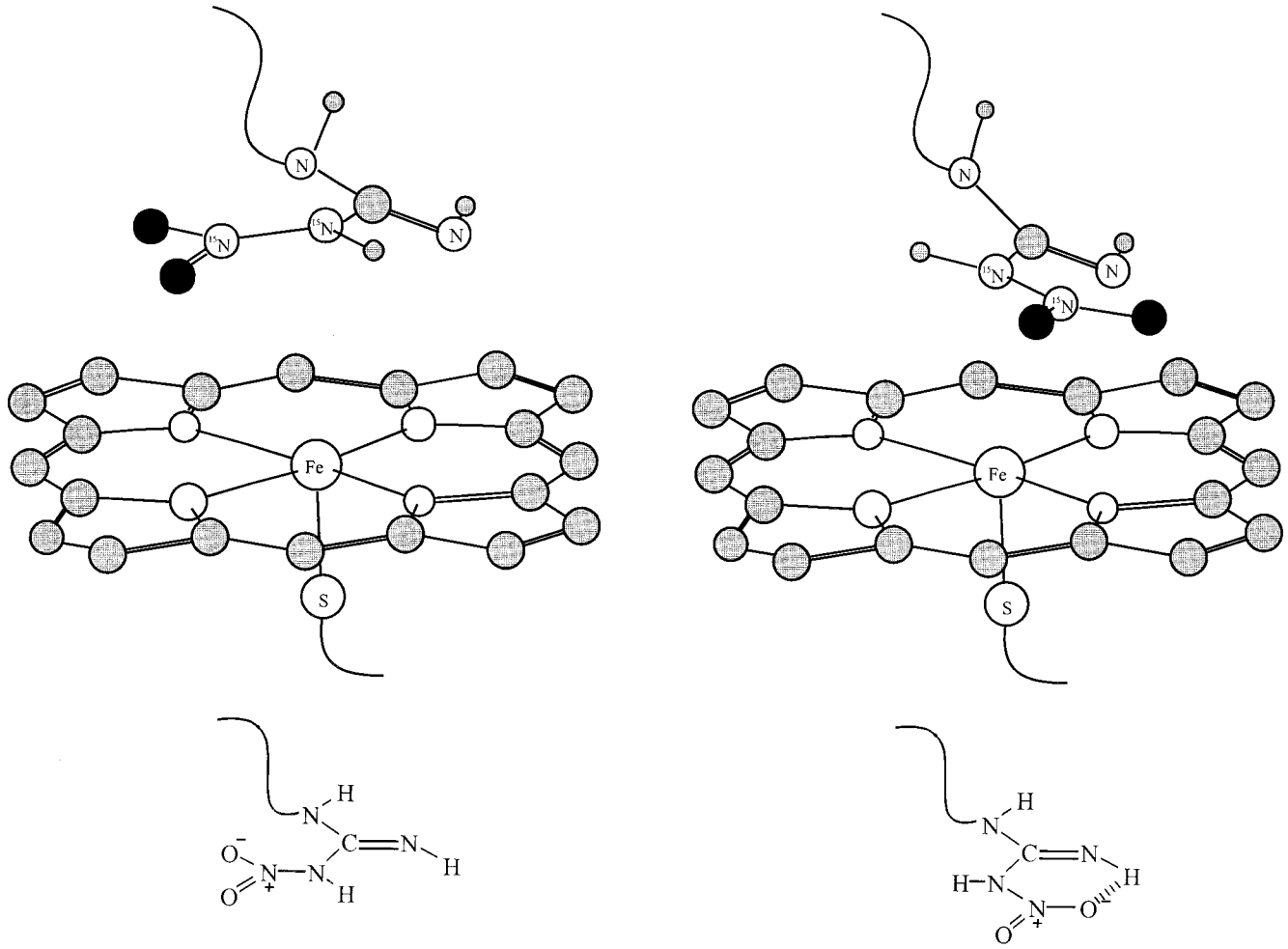

Figure 7. Three-dimensional models of Arg-NO_2 bound to nNOS based on the ENDOR-derived constraints. The two models are related by a 180° rotation about the C−N^G bond. The oxygens of Arg-NO_2 are shown in black; the protons and the central carbon of Arg-NO_2, as well as the carbons of the heme are shown in gray; the pyrrole nitrogens are shown in white. Below the simulations are corresponding structures of the nitroguanidino group.

Placement of the two nitrogens of the nitroguanidine moiety as in Scheme 2 leads to the expectation that the substituted terminal amine (NH−NO_2) of nitroarginine will show exchangeable proton signals, analogous to those reported previously for the NH-proton of NOHA's terminal NH−OH.[2] Re-Mims ^{1}H ENDOR spectra at $g_1 = 7.39$ for nitroarginine in H_2O and D_2O, shown in Figure 6, demonstrate the presence of an exchangeable proton that contributes to the inner shoulders of the outermost doublet. The coupling for this proton, clearly seen in the H_2O/D_2O difference (A−B in Figure 6, $A_1 = 2.4$ MHz, $r_{Fe-H} \approx 4.9$ Å), is 0.1−0.2 MHz smaller than that seen for NOHA. This can be considered as indicative of either a slight increase in r_{Fe-H} for the nitroarginine proton relative to NOHA, consistent with the ∼0.2 Å increase in r_{Fe-N}, or a larger displacement from the heme normal for the nitroarginine proton (see above).

The ENDOR constraints placed on the distances and orientations of $^{15}N^G$ and $^{15}N^{nitro}$, as indicated in Scheme 2 and listed in Table 1, in combination with the ENDOR constraints on the location of the $NHNO_2$ proton, significantly restrict the number of possible arrangements of nitroarginine relative to the P450-type heme. To explore the possible structures consistent with the ENDOR-derived constraints, a model of nitroarginine was constructed using the software package Chem Office (ChemDraw and Chem3D, CambridgeSoft, Cambridge, MA) and placed above an idealized model of the heme, subject to normal geometric constraints and supplemented by the ENDOR-derived constraints.[2] The two models shown in Figure 7 appear to be the only arrangements compatible with the ENDOR-derived constraints on the two ^{15}N and the ^{1}H, and are related to each other by a 180° rotation about the C−N^G bond.

Binding Geometries of LL and DD. Two-dimensional field-frequency ^{15}N ENDOR data sets obtained for the nNOS complexes of the dipeptide amides $^{15}NO_2$-**LL** and $^{15}NO_2$-**DD** also have been collected (Figure S4; $g = 4.07-6.89$). Simulation of the ^{15}N ENDOR patterns (dashed lines in Figure S4) for $^{15}NO_2$-**LL** and $^{15}NO_2$-**DD** indicate that *both* bind with the nitro nitrogen ∼4.3 Å from Fe, with Euler angles $\theta \approx 15°$, $\phi \approx 45°$. These parameters are the same as those for Arg-$^{15}NO_2$, demonstrating that both **LL** and **DD** bind to nNOS with the nitro nitrogen in the same location as that of nitroarginine.

The ^{15}N line widths at g_2 for the two dipeptides and for nitroarginine are all similar (Figure 3, Table 1), which would also *appear* to indicate that **LL** and **DD** bind in the same well-ordered geometry as nitroarginine. However, comparison of their absolute ENDOR intensities shows that $^{15}NO_2$-**LL** and Arg-$^{15}NO_2$ give approximately the same response, while the response of the $^{15}NO_2$-**DD** complex is only ∼50% that of Arg-$^{15}NO_2$ (Figure S5). The similarity of the observed line widths for the three complexes shows that the *observed* signals arise from a well-defined substate ($\Delta r \approx 0.15$ Å). We, therefore, suggest that the diminished intensity for **DD** implies that this epimer is distributed among one or more other substates—either with a

range of positions that smears out the signals, or at a slightly greater distance such that the coupling is too small to be detected (>5 Å).

As in the case of nitroarginine, the dipeptides are also expected to have an exchangeable proton very near the heme iron. The Re-Mims ^{1}H ENDOR spectra for **LL** and **DD** bound to nNOS taken at $g_1 = 7.39$ are also shown Figure 6. The **LL** epimer gives a ^{1}H spectrum similar in shape to that for nitroarginine, including a doublet with $A_1 = 2.4$ MHz that can be seen in the H/D difference (C−B in Figure 6). However, the **DD** analogue shows little evidence of shoulders inside the outermost proton doublet and does not give a well-defined H/D difference (D−B in Figure 6). Again, this likely reflects a lower degree of order for **DD**; a 50% loss in signal intensity for the **DD** proton, one that parallels the diminished ^{15}N ENDOR intensity of **DD**, could easily preclude its detection.

Discussion

The current ^{15}N and ^{1,2}H 35 GHz pulsed-ENDOR study of the binding of nitroarginine, L-Arg^{NO_2}-L-Lys-NH_2 (**LL**) and D-Lys-D-Arg^{NO_2}-NH_2 (**DD**) to holo-nNOS illustrates the application of ENDOR spectroscopy to examining the structure of non-covalently bound substrates/inhibitors. Such experiments are technically demanding because the EPR spectrum of the high-spin nNOS ferriheme shows both large g anisotropy *and* considerable *g*-strain linebroadening, in contrast to the well-defined EPR spectrum of a nitroxide[33,34] or the VO^{2+} ion.[35] The short phase memory and electronic T_1 of the high-spin ferri-nNOS EPR signal makes acquisition of pulsed-ENDOR data particularly difficult. However, the spread in field for the high spin ferriheme enhances the sensitivity of the ENDOR spectra to both distance and orientation. Analysis of complete 2D field-frequency patterns confirms that reliable distance estimates and limited orientation information can be gleaned from a small set of field dependent data around the peak of the absorption mode EPR signal (g_2). This has been demonstrated previously for both substrates, L-Arg[19] and NOHA,[2] and has been applied to all three NOS isoforms.[20] While confirming this method of analysis, the present report also shows that the angular parameters can be determined more precisely by analysis of a more complete 2D field-frequency pattern.

The ENDOR-derived constraints on the positions of N^{nitro}, N^G, and the $NHNO_2$ proton of nitroarginine lead to the two proposed structures displayed in Figure 7. These two, which are equivalent with respect to the ENDOR constraints, are related to each other by a 180° rotation about the C−N^G bond. The proximity of the two nitrogens, N^{nitro} and N^G, to the heme iron requires that the nitro group in either structure be nearly parallel to the plane of the heme: any rotation of the nitro group away from parallel quickly results in steric clash with the atoms of the porphyrin. Of the structures in Figure 7, the one on the right is particularly appealing because of the potential for stabilization through hydrogen bonding, as depicted (Figure 7). We note that this is the same conformation adopted by NOHA.[21]

The ENDOR results imply a slight repositioning of the guanidino nitrogen in nitroarginine, relative to the guanidino nitrogen of L-arginine (from 4.1 Å and ∼15° off the heme normal to 4.3 Å and almost directly above the Fe).

The EPR spectra in Figure 2 establish that **LL** and **DD** bind quantitatively to holo-nNOS, while the ENDOR spectra in Figure 3 and **S3** establish that the nitro groups of both **LL** and its *retro-inverso* analogue,[11,12] **DD**, bind close to the heme iron of holo-nNOS. Analysis of the ENDOR data shows that the nitro nitrogen of each dipeptide (Figure 3) is at the same distance from the heme iron as that of nitroarginine, 4.3 Å. The ^{15}N spectra for $^{15}NO_2$-**LL** and $^{15}NO_2$-**DD** are nearly identical to each other and to that of nitroarginine, which indicates that nitroarginine and the two inhibitors *all* bind with the nitroguanidine moiety in the same location "above" the heme iron. Clearly, the ENDOR data establish the binding modes for **LL** and **DD** shown in Figure 1.

The sharp-line ^{15}N spectra observed at g_2 for all of the substrates and inhibitors (e.g., Figure 3) further give the impression that all of them bind to holo-nNOS in a well ordered fashion, with the observed ENDOR intensities coming from substrate molecules with a distribution in r of no more than $\Delta r \approx 0.15$ Å. However, on the basis of differences in the absolute Mims pulsed-ENDOR intensities, we suggest that nitroarginine and the **LL** epimer bind almost exclusively in the geometries described, but that the **DD** epimer binds in multiple substates. It appears that as little as ∼50% of the **DD** molecules reside in the well-defined geometry exhibited by the other two, while the rest are either distributed over a range of distances or are at a slightly greater distance, and not detected. This supposition is supported by the appearance of the ^{1}H ENDOR at g_1 in Figure 6.

Thus, the ENDOR data support the proposed rationalization for the holo-nNOS selectivities of **LL** and **DD** shown in Figure 1, while disclosing subtle differences in the binding of the two epimers. This is the first spectroscopic evidence to support the model shown in Figure 1[6] and suggested previously[11−15] for how *retro-inverso* peptides bind to enzymes.

Acknowledgment. We acknowledge the instrumental efforts of Mr. Clark Davoust. We are grateful to the National Institutes of Health for financial support of this work to R.B.S. (GM 49725) and B.M.H. (HL 13531).

Supporting Information Available: Syntheses of L- and D-[^{15}N]nitroarginine, [$^{15}NO_2$]-**LL**, and [$^{15}NO_2$]-**DD**; five figures showing pyrrole ^{14}N CW ENDOR for nitroarginine-bound nNOS (Figure S1); absolute intensity comparisons at g_1 and g_2 for ^{15}N-Arg-$^{15}NO_2$, Arg-$^{15}NO_2$, and their difference, (^{15}N-Arg-$^{15}NO_2$) − (Arg-$^{15}NO_2$) (Figure S2); field-dependent ^{15}N ENDOR spectra for ^{15}N-Arg-$^{15}NO_2$, Arg-$^{15}NO_2$, and their difference (g = 4.19−7.39, Figure S3); field-dependent ^{15}N ENDOR data for **LL** and **DD** (g = 4.07−6.89, Figure S4); and overlaid normalized ENDOR spectra for Arg-$^{15}NO_2$, $^{15}NO_2$-**LL** and $^{15}NO_2$-**DD** at $g_2 = 4.28$ (Figure S5) along with one supporting table (Table S1) describing fits to the data for ^{15}N-Arg-$^{15}NO_2$ (PDF). This material is available free of charge via the Internet at http://pubs.acs.org.

JA993927B

(33) Mustafi, D.; Knock, M. M.; Shaw, R. W.; Makinen, M. W. *J. Am. Chem. Soc.* **1997**, *119*, 12619−12628.

(34) Mustafi, D.; Makinen, M. W. *J. Am. Chem. Soc.* **1995**, *117*, 6739−6746.

(35) Mustafi, D.; Telser, J.; Makinen, M. W. *J. Am. Chem. Soc.* **1992**, *114*, 6219−6226.